PROCEEDINGS OF SPIE

SPIEDigitalLibrary.org/conference-proceedings-of-spie

Reconfigurable dynamic optical system design, test, and data analysis

Kim, Dae Wook, Aftab, Maham, Trumper, Isaac, Graves, Logan, Quach, Henry, et al.

Dae Wook Kim, Maham Aftab, Isaac Trumper, Logan Graves, Henry Quach, Hyukmo Kang, Hyemin Yoo, Andrew Lowman, Greg Smith, Matt Dubin, Chang-Jin Oh, Justin Hyatt, Christian Davila-Peralta, Heejoo Choi, "Reconfigurable dynamic optical system design, test, and data analysis," Proc. SPIE 11352, Optics and Photonics for Advanced Dimensional Metrology, 1135202 (7 April 2020); doi: 10.1117/12.2555650

Event: SPIE Photonics Europe, 2020, Online Only, France

Invited Paper

Reconfigurable dynamic optical system design, test, and data analysis

Dae Wook Kim[*a,b], Maham Aftab[a], Isaac Trumper[a,c], Logan Graves[a,c], Henry Quach[a], Hyukmo Kang[a], Hyemin Yoo[a], Andrew Lowman[a], Greg Smith[a], Matt Dubin[a], Chang-jin Oh[a], Justin Hyatt[b], Christian Davila-Peralta[b], Heejoo Choi[a]

[a]Wyant College of Optical Sciences, University of Arizona, 1630 E. University Blvd., Tucson, AZ 85721, USA
[b]Department of Astronomy and Steward Observatory, University of Arizona, 933 N. Cherry Ave., Tucson, AZ 85719, USA
[c]ELE Optics, 405 E. Wetmore Ste 117-260, Tucson, AZ 85705, USA

ABSTRACT

Reconfigurable freeform optical systems enable greatly enhanced imaging and focusing performance within non-symmetric, compact, and ergonomic form factors. In this paper, several improvements are presented for the design, test, and data analysis with these systems. Specific improvements include definition of a modal **G** and **C** vector basis set based on Chebyshev polynomials for the design and analysis of non-circular optical systems. This framework is then incorporated into a parametric optimization process and tested with the Tomographic Ionized-carbon Mapping Experiment (TIME), a reconfigurable optical system. Beyond design, a reconfigurable deflectometry system enhances metrology to measure a fast, f/1.26 convex optic as well as an Alvarez lens. Further improvements in an infrared deflectometry system show accuracy around $\lambda/10$ of the notoriously difficult low-order power. Working together, the mathematical vector polynomial set, the programmatic optical design approach, and various deflectometry-based optical testing technologies enable more flexible and optimal utilization of freeform optical components and design configurations.

Keywords: Freeform optics, Vector Polynomials, Parametric Optimization, **G** Polynomials, **C** Polynomials, Fitness Function, Deflectometry, Infrared Deflectometry

1. INTRODUCTION

Increasingly sophisticated optics are being developed for various fields such as astronomy, commercial photography, industrial manufacturing, and medical imaging. To aid in the design, testing, and analysis of these systems, this paper presents tools based on or designed for reconfigurable dynamic optical systems.

First, this paper mathematically defines an orthonormal gradient and curl polynomial basis set, designed for high accuracy modeling of non-circular wavefronts in the presence of defects and noise. These modal vector basis sets, called the **G** and **C** polynomials, are derived from gradients and curls of the Chebyshev polynomials of the first kind.

Fitting wavefronts to mathematical models is useful for parametric optimization for freeform optical design. To this end, this paper develops a model to perform such optimization and demonstrates its utility with the Tomographic Ionized-carbon Mapping Experiment (TIME) which contains reconfigurable optical elements.

Extending beyond optical design, this paper illustrates enhanced optical metrology tools for fabricating challenging freeform mirrors. Two recent developments are presented here: 1) The first uses a reconfigurable deflectometry setup to measure a fast, f/1.26 convex optic as well as an Alvarez lens. Independent verification of these surface measurements highlights the ability of this system to characterize optical elements not easily processed with traditional metrology systems. 2) Lastly, this paper pushes the envelope of accuracy with an infrared deflectometry system used to measure a 6.5m mirror. With careful elimination of systematic errors, accuracy is demonstrated to approximately $\lambda/15$ accuracy for higher order terms.

Taken together, this paper demonstrates design tools for reconfigurable optical systems as well as reconfigurable optical test and data analysis techniques to improve optical metrology.

*letter2dwk@hotmail.com

Optics and Photonics for Advanced Dimensional Metrology, edited by Peter J. de Groot, Richard K. Leach, Pascal Picart
Proc. of SPIE Vol. 11352, 1135202 · © 2020 SPIE · CCC code: 0277-786X/20/$21 · doi: 10.1117/12.2555650

2. ORTHONORMAL RECTANGULAR DOMAIN VECTOR POLYNOMIALS

2.1 Modal data processing of vector distribution

As increasingly advanced fabrication methods for optics are developed, especially for high-resolution or freeform designs, optical metrology and analysis must be more precise, efficient and robust, and data processing from these should be faster, more efficient and reliable.

Modal data processing is routinely employed in surface and wavefront reconstruction. For high-resolution and freeform optics, it is often the desired method but not always practical as many common orthonormal modal data sets are limited by complex generation functions, loss of orthogonality in the vector domain, etc. We have developed a vector based polynomial basis set, derived from two dimensional (2D) Chebyshev polynomials, orthonormal in the rectangular domain. This is a combination of two sets – **G** polynomials [1] that can represent gradient or slope data and **C** polynomials [2] that can fit curl or rotational data. Both of these sets are orthonormal across rectangular apertures. If the common Laplacian terms are only included once, these two sets together can be used to fit any vector data in the rectangular domain. Some of their properties that make them very attractive for data fitting include:

1) The scalar basis set (2D Chebyshev polynomials), as well as the vector sets (**G** and **C** polynomials) are orthonormal in the rectangular domain.

2) The vector sets can be derived straightforwardly from the scalar sets without needing any orthogonalization techniques, such as Gram-Schmidt orthogonalization.

3) It is possible and computationally simple to generate several thousands of polynomials which makes them ideal for representing freeform and high-resolution surfaces.

2.2 G and C vector polynomials

Chebyshev polynomials of the first kind can be defined as:

$$\begin{aligned} &T_{m+1}(x) = 2xT_m(x) - T_{m-1}(x) \\ &\text{where } T_0(x) = 1,\ \ T_1(x) = x,\ \text{for} -1 \le x \le 1 \end{aligned} \tag{1}$$

Two-dimensional Chebyshev polynomials can then be written as:

$$F_j(x,y) = F_n^m(x,y) = T_m(x)T_n(y) \tag{2}$$

We define the G and C polynomials [1, 2] from the equations:

$$\begin{aligned} \vec{G}_j(x,y) = \vec{G}_n^m(x,y) = \nabla F_n^m(x,y) &= \frac{\partial}{\partial x}F_n^m(x,y)\hat{i} + \frac{\partial}{\partial y}F_n^m(x,y)\hat{j} \\ &= T_n(y)T_m'(x)\hat{i} + T_m(x)T_n'(y)\hat{j} \end{aligned} \tag{3}$$

$$\begin{aligned} \vec{C}_j(x,y) = \vec{C}_n^m(x,y) &= \frac{\partial}{\partial y}F_n^m(x,y)\hat{i} - \frac{\partial}{\partial x}F_n^m(x,y)\hat{j} \\ &= T_m(x)T_n'(y)\ \hat{i} - T_n(y)T_m'(x)\ \hat{j} \end{aligned} \tag{4}$$

In general, the polynomial sets are defined in the Cartesian coordinate system, with [x, y] axes. Terms *m* and *n* are indices of polynomial functions in x and y respectively. They are both variables with positive integer values that go from 0 to infinity. They are used to denote the order of the polynomial. For 2D polynomials, an additional variable, *j*, is introduced that denotes the order of the polynomial, in the same way that *m* and n denote polynomial order for 1D polynomials. Since the 2D polynomials are a function of 1D polynomials, *j* can be written in terms of *m* and *n* and this relation is described in reference [1]. The terms $\hat{\imath}$ and $\hat{\jmath}$ are the unit vectors in the x and y directions, respectively. The terms with ′ are gradients e.g., T′(x) is the gradient of T in the x dimension.

3. FITNESS FUNCTION BASED FREEFORM DESIGN

3.1 Fitness function-based freeform optical system design

When evaluating a design to determine if breaking rotational symmetry and employing freeform surfaces is worth the effort, a data-driven methodology should be employed. The decision to increase the number of degrees of freedom through freeform surfaces can yield reduced volume, increased field of view (FOV), or increased imaging performance, but typically comes at a high cost. Therefore, we need to carefully choose to which surfaces we apply freeform terms in order to maximize their impact. To guide this selection process, we developed a parametric fitness function using modal wavefront fitting [3, 4]. The fitness function combines multiple metrics from aberration control to manufacturability to provide a single data-driven metric. Equation 5 is one form of the fitness function that we propose,

$$f = w_1 U_{fr} - w_2 \sqrt{\left(\Delta S_f^{RMS}\right)^2 + (\Delta S_r^{RMS})^2} + w_3 \Delta S_x^{RMS} + w_4 \Delta S_y^{RMS} - w_5 F_\Delta^{PSD}, \tag{5}$$

where U_{fr} is the minimum fractional overlap between the forward (f) and the reverse (r) data, which captures the input data quality; ΔS_f^{RMS} and ΔS_r^{RMS} are parameters capturing how well a single surface represents the ensemble of all input data at the surface; ΔS_x^{RMS} and ΔS_y^{RMS} are parameters that capture the amount of potential aberration correction over the entire FOV at the surface; and F_Δ^{PSD} is the parameter to represent the difficulty manufacturing the surface. Each parameter set has its own unique weight and sums together to provide a single metric to evaluate the surface, where a large positive value of the function is optimal.

The data that we use to inform the selection comes from forward and reverse ray trace data at every surface of interest within the design. An aberrated optical system will have discrepancies between these data, while a non-aberrated system will have identical data, as shown in Figure 1. The typical goal of optimization is to take an aberrated system and turn it into a non-aberrated system. Therefore, throughout the process of optimization, as more freeform terms are employed, the data input into the fitness function will converge.

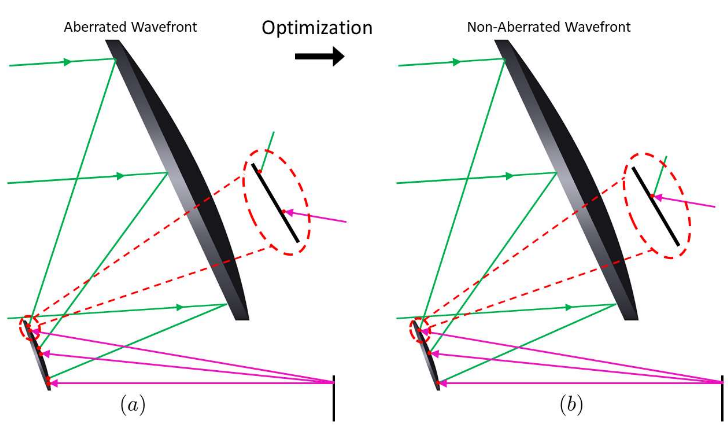

Figure 1. Forward (green) and reverse (magenta) ray data is used as the input to the parametric fitness function. As optimization converges to a local minimum, the aberrations in the system are reduced and the two data sets converge as shown in the call-out. [3, 4]

3.2 TIME instrument design using dynamic K-mirror optical configuration

To validate its efficiency, the parametric fitness function was employed on a real-world project, the Tomographic Ionized-carbon Mapping Experiment (TIME) including a reconfigurable dynamic (i.e., rotating to de-rotate the field on sky) K-mirror configuration. Shown in Figure 2 is an optical design performed in Zemax that utilized freeform surfaces on K2, P1, P2, and C1 to enable a linear FOV mm-wave experiment on the 12-meter ALMA prototype radio telescope on Kitt Peak in Arizona.

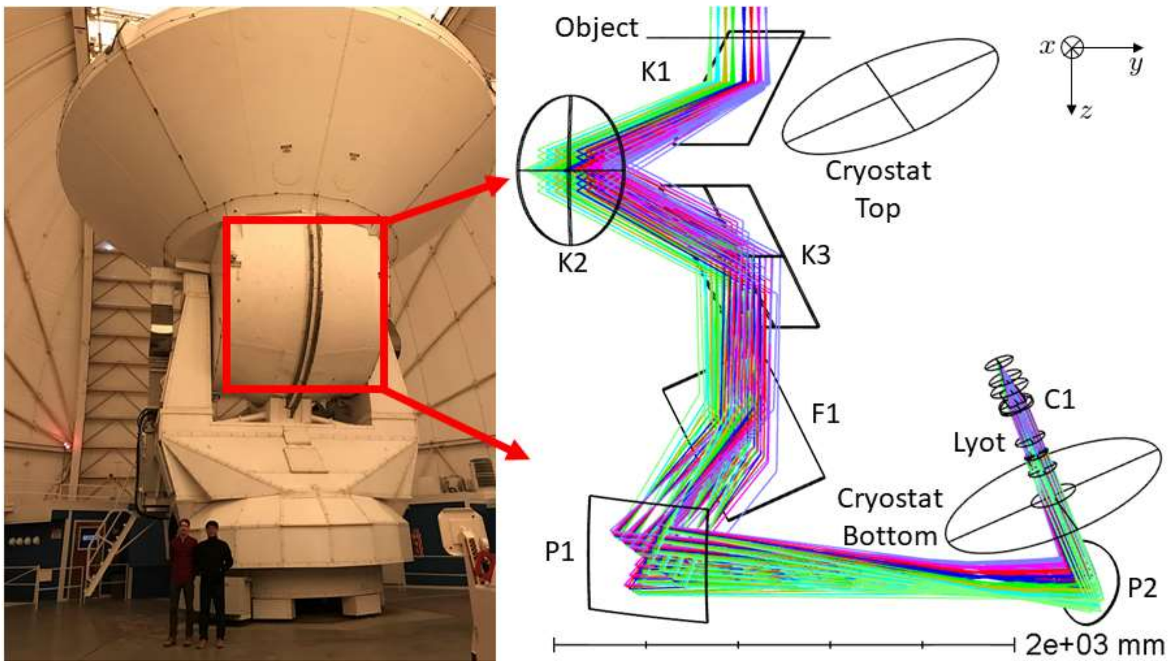

Figure 2. The 12-meter ALMA prototype radio telescope (left) on Kitt Peak in Arizona with its cabin called out, which houses the Tomographic Ionized-carbon Mapping Experiment (TIME) (right). The TIME optical design required an extremely folded beam path to fit the large linear FOV and cryostat in the defined volume of the telescope cabin. [3, 4]

4. FREEFORM OPTICS METROLOGY AND ANALYSIS

Reconfigurable dynamic optical systems often utilize highly aspheric or freeform optics to balance the optical aberration or performance merits for all possible configurations since their optical configurations are usually off-axis or axially non-symmetric. Thus, high dynamic range precision non-null freeform optics metrology becomes an essential technology to manufacture such reconfigurable optical systems (e.g., TIME instrument in Section 3.2).

Historically, deflectometry has only been utilized for testing concave surfaces, or smaller flat optics; this is due to the nature of deflectometry, which requires that a source area is large enough to satisfy a ray path from the source to the full optical aperture area under test, and then into a camera after reflection. For extremely large optical surfaces, such as the 8.4-meter Giant Magellan Telescope primary mirror segments, the required source area can be quite reasonable if the source and camera are placed near the center of curvature of the optic.

4.1 Infinite deflectometry for flat and convex freeform optics

For convex optics, placing the source and camera near this location becomes impossible and if a planar source is used, as is traditional, the required source area can range from very large to infinitely large depending on the surface curvature. To solve the issue of testing challenging optics such as convex optics using deflectometry, a methodology known as infinite deflectometry was created, which achieves a 2π steradian measurement volume. [5]

Infinite deflectometry achieves its wide testing range by creating a virtual source enclosure around the test optic. To do this, a source is tilted to create a ramp over the test optic, and a camera is mounted facing down towards the optic. In this configuration, a portion of the optic under test is measurable. To close the loop and measure the full aperture, the test optic is mounted on a precision rotation stage and clocked a fixed interval, which creates a new 'virtual' deflectometry system at each angular position. By sweeping through the full 2π rotation, screens of the virtual systems create a 'tipi' source enclosure around the optic under test and allow for testing a wide range of surface slopes, from concave to convex. The basic principle of the infinite deflectometry system, from the physical hardware to the virtual source enclosure, is shown in Figure 3.

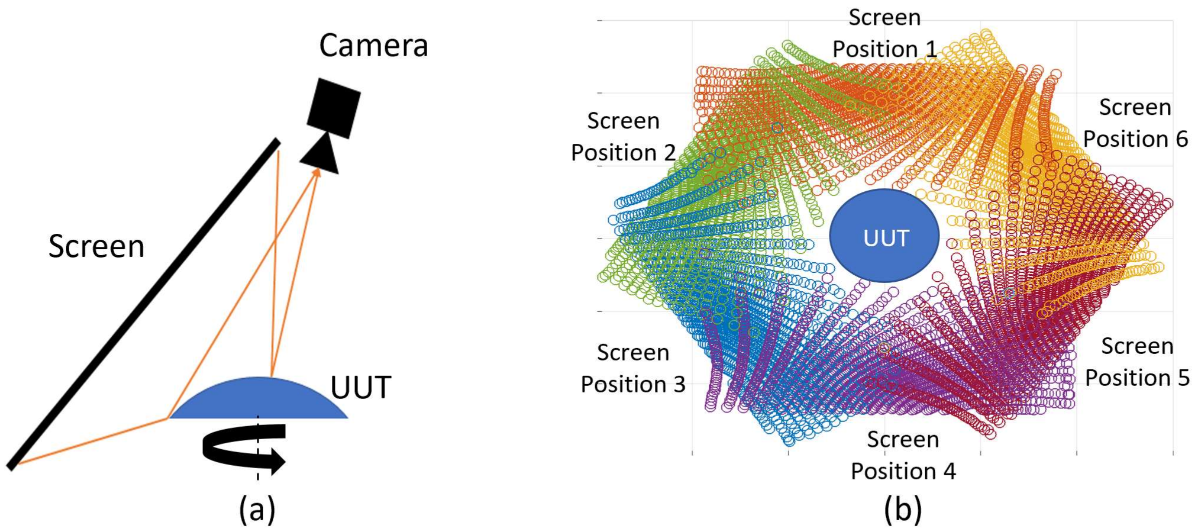

Figure 3. Tilting a planar source screen over a convex optic under test allows for measuring a slice of the optical surface(a). By placing the Unit Under Test (UUT) on a precision rotation stage, the surface can be clocked at fixed intervals through a full rotation. In effect, a new virtual screen and camera are created at each rotated position. The collection of virtual sources creates a 2π steradian measurement volume enclosing the UUT allowing for the same precision metrology over the full UUT aperture (b). [5]

The infinite deflectometry system has been used to successfully test both fast convex optics and highly freeform optical surfaces. In one test scenario that presents a common challenge in metrology, a fast F/1.26 large convex optic with 50 mm diameter was measured using both an infinite deflectometry system and a commercial interferometer.

Since the interferometer was unable to measure the full aperture of the convex optic in a single shot configuration, the reconstructed surface maps of the 43 mm diameter common aperture were used for comparison, with the standard Zernike terms 1:4, 1:6, 1:21, and 1:37 removed. The results demonstrated a strong match between both test methods across all spatial frequencies. After removing Zernike terms 1:37, the interferometer reported 18.48 nm RMS surface height while the infinite deflectometry reconstruction reported 16.26 nm RMS, demonstrating the system can achieve optical quality testing for large, fast, convex optics.

For a more challenging test, a highly freeform Alvarez lens was measured using the infinite deflectometry system. Because no null optic was available for this surface, and the fringe density with a spherical null exceeded the range of the available commercial interferometers, the surface was cross checked using a KLA-Tencor Alpha-Step D-500 profilometer. The profilometer profile measurement, S_P, and the height of the same profile taken from the Alvarez infinite deflectometry map, are reported. The results of the infinite deflectometry reconstruction, the designed Alvarez lens, and the profilometer measurements are shown in Figure 4.

With these tests, the infinite deflectometry method has proven to be a viable test solution and expands deflectometry to providing optical quality testing for convex optics and highly freeform optics which are traditionally challenging to test.

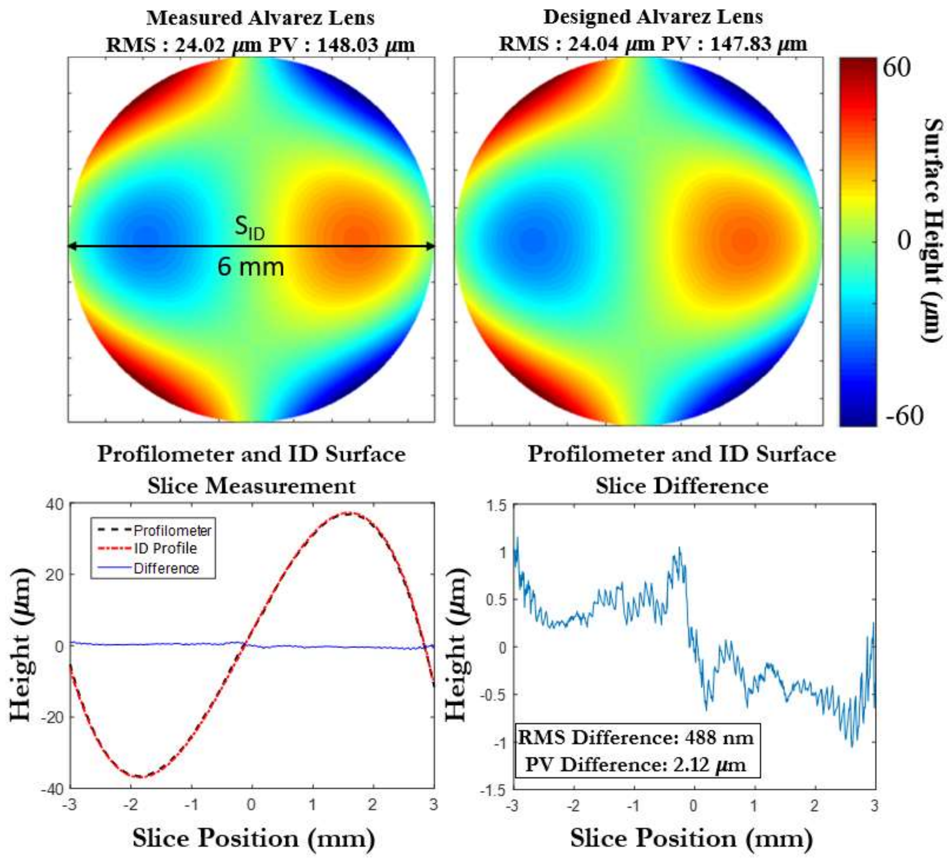

Figure 4. An Alvarez lens, a highly freeform optic, was designed with a 6 mm diameter aperture with 17 μm of horizontal coma and -17 μm of trefoil (top right) and manufactured. The final surface generated was measured using the Infinite Deflectometry (ID) system (top left). To cross check the infinite deflectometry result, a profilometer measurement of a slice of the surface was compared to the same slice from the infinite deflectometry reconstruction map, S_{ID} (shown as a black line in the surface map) (top left). The surface height of the profile from the infinite deflectometry measurement and the profilometer were compared (bottom left) and the Peak-to-Valley difference was found to be 1.48% of the total PV height across the 6 mm diameter. [5]

4.2 Infrared non-null deflectometry for astronomical mirror shape analysis

One key to the successful implementation of freeform optics is to consider the challenges of manufacturing such as testing. Deflectometry is a versatile approach to metrology that has a large dynamic range with low uncertainty. [6] Early in the fabrication process, an infrared deflectometry system allows for figuring while grinding. [7] This greatly reduces the cost and time for fabricating freeform optics.

Infrared deflectometry has been used to make non-rotationally symmetrical optics, and it accurately guided the grinding process. [8] Demonstrations of an optic's figure converging towards the desired shape show the usefulness of infrared deflectometry, but understanding the uncertainty in the measurement is important. To do this it is necessary to compare the deflectometry measurements to another metrology system that is reliable. This was done with a 6.5 m diameter, rotationally symmetrical conic mirror. [9]

Figure 5 shows the difference between the deflectometry and interferometric data. The RMS difference is 0.73 μm, and most of this is power. When power is removed, the total error is 0.33 μm. We also looked at the high order errors. To do this, we subtracted the first 37 Zernike terms from the discrepancy between deflectometry and interferometry. This data has an RMS value of 0.04 μm. While there are some artifacts with 30 degree spacing due to the clocking of the mirror during testing, the residual is quite small. This shows that infrared deflectometry can accurately measure mid spatial frequencies.

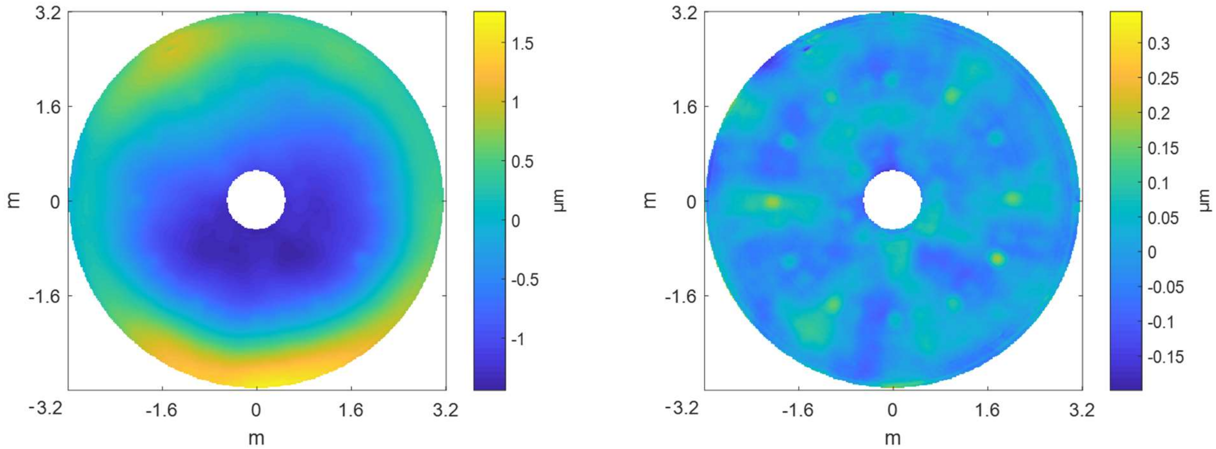

Figure 5. The difference between the final averaged surface error maps of the infrared deflectometry (including thermal bending correction) and null interferometry (including coma correction) having the RMS error of 0.73 µm (left) and the residual of the difference map with 37 Zernike terms removed having an error of 0.04 µm RMS (right).

Infrared deflectometry has also been used to measure metal reflectors that are diffuse at optical wavelengths, like those used in radio telescopes [10], and efforts to utilize it as closed-loop feedback in automated manufacturing systems are under development [11].

5. CONCLUDING REMARKS

Highly flexible and dynamic optical systems such as the TIME instrument [3, 4] and compact mobile ultra-zoom lens systems promise to be key enablers for future scientific discoveries in astronomy and to revolutionize consumer optics applications. To achieve the required performance, novel design choices, optimization, metrology, and data analysis are being made at all levels of the advanced systems. [12 – 14] These dynamic optical systems with reconfigurable optical layouts will require further innovations across many disciplines and collaboration among many scientists and engineers. Our team at the University of Arizona continues to push the limits by improving accuracy, precision, robustness, dynamic range, and data analysis solutions.

REFERENCES

[1] Aftab, M., Burge, J.H., Smith, G.A. et al. Modal Data Processing for High Resolution Deflectometry. Int. J. of Precis. Eng. and Manuf.-Green Tech. 6, 255–270 (2019).
[2] Aftab, M., Graves, L.R., Burge, J.H., Smith, G.A., Oh, C,J, Kim, D.W., "Rectangular domain curl polynomial set for optical vector data processing and analysis," Opt. Eng. 58(9) 095105 (2019).
[3] Trumper, I. L., Marrone, D. P., and Kim, D. W., "Utilizing freeform optics in dynamic optical configuration designs," Journal of Astronomical Telescopes, Instruments, and Systems 5(3), 035005 (12 July 2019).
[4] Trumper, I. L., Aftab, M., and Kim, D. W., "Freeform surface selection based on parametric fitness function using modal wavefront fitting," Opt. Express 27, 6815-6831 (2019).
[5] Graves, L. R., Quach, H., Choi, H., and Kim, D. W., "Infinite deflectometry enabling 2π-steradian measurement range," Opt. Express 27, 7602-7615 (2019).
[6] Su, P., Parks, R. E., Wang, L., Angel, R. P. and Burge, J. H., "Software configurable optical test system – computerized reverse Hartmann test". Applied Optics. Vol. 49, No. 25(2010).
[7] Su, T., Park, W. H., Parks, R. E., Su, P., & Burge, J. H., "Scanning long-wave optical test system - A new ground optical surface slope test system". Proc. SPIE 8126, (2011).
[8] Oh, C., et al. "Fabrication and Testing of 4.2m Off-Axis Aspheric Primary Mirror of Daniel K. Inouye Solar Telescope". Proc. SPIE 9912, (2016).

[9] Yoo, H., Smith, G., Oh, C., Lowman, A., Dubin, M., “Improvements in the scanning long-wave optical test system”. Proc. SPIE 10742, (2018).

[10] Graves, L. R., Quach, H., Koshel, R. J., Oh, C., and Kim, D. W., "High contrast thermal deflectometry using long-wave infrared time modulated integrating cavity source," Opt. Express 27, 28660-28678 (2019).

[11] Hyatt, J. and Davila-Peralta, C., “A Rapid and Adaptable Method for Manufacturing High-Accuracy Antenna Reflectors”, Radio/Millimeter Astro. Front. in the Next Decade (2019).

[12] Graves, L. R., Smith, G. A., Apai, D., and Kim, D. W., "Precision Optics Manufacturing and Control for Next-Generation Large Telescopes," Nanomanufacturing and Metrology 2(2), 65-90 (2019).

[13] Trumper, I., Anderson, A. Q., Howard, J. M., West, G., Kim, D. W., "Design form classification of two-mirror unobstructed freeform telescopes," Opt. Eng. 59(2), 025105 (2020).

[14] Trumper, I., Hallibert, P., Arenberg, J., Kunieda, H., Guyon, O., Stahl, H. P., and Kim, D. W., "Optics technology for large-aperture space telescopes: from fabrication to final acceptance tests," Adv. Opt. Photon. 10, 644-702 (2018).